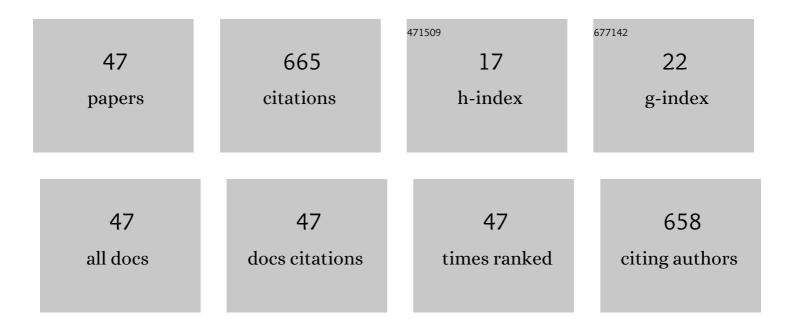
## Hui Sun

List of Publications by Year in descending order

Source: https://exaly.com/author-pdf/5207797/publications.pdf Version: 2024-02-01



Ητιί Stin

#	Article	IF	CITATIONS
1	Effect of annealing temperature on the optoelectronic properties and structure of NiO films. Ceramics International, 2022, 48, 2820-2825.	4.8	18
2	Highly transparent and conductive p-type Cul films by optimized solid-iodination at room temperature. Nanotechnology, 2022, 33, 105706.	2.6	6
3	High power impulse magnetron sputtering growth processes for copper nitride thin film and its highly enhanced UV - visible photodetection properties. Journal of Alloys and Compounds, 2022, 896, 162924.	5.5	8
4	Periodic mesoporous organosilica coupled with chlorin e6 and catalase for enhanced photodynamic therapy to treat triple-negative breast cancer. Journal of Colloid and Interface Science, 2022, 610, 634-642.	9.4	8
5	Pico-molar level detection of copper ion with extraordinarily high response by Ti-doped copper nitride fabricated via high power impulse magnetron sputtering. Sensors and Actuators B: Chemical, 2022, 360, 131632.	7.8	3
6	Research Progress of p-Type Oxide Thin-Film Transistors. Materials, 2022, 15, 4781.	2.9	11
7	Review in optoelectronic properties of p-type CuCrO2 transparent conductive films. Surfaces and Interfaces, 2021, 22, 100824.	3.0	18
8	Optoelectronic properties of an AZO/Ag multilayer employed as a flexible electrode. Ceramics International, 2021, 47, 5671-5676.	4.8	19
9	Influence of carbon content on the mechanical properties of TiCN–Cu nanocomposite coatings prepared by multi-arc ion plating. Vacuum, 2021, 187, 110139.	3.5	18
10	Tuning the Electrical Properties of NiO Thin Films by Stoichiometry and Microstructure. Coatings, 2021, 11, 697.	2.6	1
11	Influence of annealing temperature on the optoelectronic properties of ITZO thin films. Nanotechnology, 2021, 32, 405701.	2.6	2
12	Research Progress of Transparent Electrode Materials with Sandwich Structure. Materials, 2021, 14, 4097.	2.9	6
13	In-Sn-Zn Oxide Nanocomposite Films with Enhanced Electrical Properties Deposited by High-Power Impulse Magnetron Sputtering. Nanomaterials, 2021, 11, 2016.	4.1	4
14	Optoelectronic properties of p-type NiO films deposited by direct current magnetron sputtering versus high power impulse magnetron sputtering. Applied Surface Science, 2020, 508, 145106.	6.1	30
15	Structure, mechanical and tribological properties, and oxidation resistance of TaC/a-C:H films deposited by high power impulse magnetron sputtering. Ceramics International, 2020, 46, 24986-25000.	4.8	14
16	Mechanical properties, thermal stability and oxidation resistance of HfC/a-C:H films deposited by HiPIMS. Journal of Alloys and Compounds, 2020, 847, 156538.	5.5	10
17	p-type semi-transparent conductive NiO films with high deposition rate produced by superimposed high power impulse magnetron sputtering. Ceramics International, 2020, 46, 27695-27701.	4.8	10
18	Transparent Conductive p-Type Cuprous Oxide Films in Vis-NIR Region Prepared by Ion-Beam Assisted DC Reactive Sputtering. Coatings, 2020, 10, 473.	2.6	9

Ниі Ѕим

#	Article	IF	CITATIONS
19	The Optoelectronic Properties of p-Type Cr-Deficient Cu[Cr0.95â^'xMg0.05]O2 Films Deposited by Reactive Magnetron Sputtering. Materials, 2020, 13, 2376.	2.9	6
20	Research on adhesion strength and optical properties of SiC films obtained via RF magnetron sputtering. Chinese Journal of Physics, 2020, 64, 79-86.	3.9	10
21	Influence of power frequency on the performance of SiC thin films deposited by pulsed DC magnetron sputtering. Journal of Adhesion Science and Technology, 2019, 33, 2181-2190.	2.6	7
22	Influence of Sputtering Power on the Electrical Properties of In-Sn-Zn Oxide Thin Films Deposited by High Power Impulse Magnetron Sputtering. Coatings, 2019, 9, 715.	2.6	6
23	Contribution of enhanced ionization to the optoelectronic properties of p-type NiO films deposited by high power impulse magnetron sputtering. Journal of the European Ceramic Society, 2019, 39, 5285-5291.	5.7	17
24	Comparison of microstructural and optoelectronic properties of NiO:Cu thin films deposited by ion-beam assisted rf sputtering in different gas atmospheres. Thin Solid Films, 2019, 677, 103-108.	1.8	8
25	Optoelectronic properties of Cu3N thin films deposited by reactive magnetron sputtering and its diode rectification characteristics. Journal of Alloys and Compounds, 2019, 789, 428-434.	5.5	29
26	Enhanced photocatalytic activity by photo-Fenton reaction: towards TiO <sub>2</sub> nanotubes sensitized by Fe(III)-tartrate. Journal Physics D: Applied Physics, 2019, 52, 175302.	2.8	2
27	Light enhanced moisture degradation of perovskite solar cell material CH <sub>3</sub> NH <sub>3</sub> Pbl <sub>3</sub> . Journal of Materials Chemistry A, 2019, 7, 27469-27474.	10.3	37
28	Electrical and magnetic properties of (Al, Co) co-doped ZnO films deposited by RF magnetron sputtering. Surface and Coatings Technology, 2019, 359, 390-395.	4.8	20
29	The adhesion strength and mechanical properties of SiC films deposited on SiAlON buffer layer by magnetron sputtering. Surface and Coatings Technology, 2019, 360, 116-120.	4.8	10
30	Synthesis and characterization of n-type NiO:Al thin films for fabrication of p-n NiO homojunctions. Journal Physics D: Applied Physics, 2018, 51, 105109.	2.8	13
31	High transmittance in IR region of conductive ITO/AZO multilayers deposited by RF magnetron sputtering. Ceramics International, 2018, 44, 6769-6774.	4.8	27
32	Impact of active layer thickness of nitrogen-doped In–Sn–Zn–O films on materials and thin film transistor performances. Journal Physics D: Applied Physics, 2018, 51, 175101.	2.8	13
33	p-type conductive NiOx: Cu thin films with high carrier mobility deposited by ion beam assisted deposition. Ceramics International, 2018, 44, 3291-3296.	4.8	18
34	The Influence of Oxygen Flow Ratio on the Optoelectronic Properties of p-Type Ni1â^'xO Films Deposited by Ion Beam Assisted Sputtering. Coatings, 2018, 8, 168.	2.6	12
35	p-type cuprous oxide thin films with high conductivity deposited by high power impulse magnetron sputtering. Ceramics International, 2017, 43, 6214-6220.	4.8	25
36	Microstructures and optoelectronic properties of nickel oxide films deposited by reactive magnetron sputtering at various working pressures of pure oxygen environment. Ceramics International, 2017, 43, S369-S375.	4.8	30

Hui Sun

#	Article	IF	CITATIONS
37	Thickness-dependent optoelectronic properties of CuCr0.93Mg0.07O2 thin films deposited by reactive magnetron sputtering. Materials Science in Semiconductor Processing, 2017, 63, 295-302.	4.0	12
38	The electrical stability of In-doped ZnO thin films deposited by RF sputtering. Journal Physics D: Applied Physics, 2017, 50, 045102.	2.8	10
39	Ag composition gradient CuCr0.93Mg0.07O2/Ag/CuCr0.93Mg0.07O2 coatings with improved p-type optoelectronic performances. Journal of Materials Science, 2017, 52, 11537-11546.	3.7	14
40	Absorption Amelioration of Amorphous Si Film by Introducing Metal Silicide Nanoparticles. Nanoscale Research Letters, 2017, 12, 224.	5.7	5
41	High photodegradation ability of dyes by Fe(III)-tartrate/TiO2 nanotubular photocatalyst supported via photo-Fenton reaction. Journal of Photochemistry and Photobiology A: Chemistry, 2017, 334, 20-25.	3.9	18
42	Optoelectronic Properties and the Electrical Stability of Ga-Doped ZnO Thin Films Prepared via Radio Frequency Sputtering. Materials, 2016, 9, 987.	2.9	14
43	Optoelectronic properties of delafossite structure CuCr <sub>0.93</sub> Mg <sub>0.07</sub> O <sub>2</sub> sputter deposited coatings. Journal Physics D: Applied Physics, 2016, 49, 185105.	2.8	26
44	Microstructures and optoelectronic properties of CuxO films deposited by high-power impulse magnetron sputtering. Journal of Alloys and Compounds, 2016, 688, 672-678.	5.5	22
45	Towards delafossite structure of Cu–Cr–O thin films deposited by reactive magnetron sputtering: Influence of substrate temperature onÂoptoelectronics properties. Vacuum, 2015, 114, 101-107.	3.5	22
46	Modification of TiO2 nanotubes by WO3 species for improving their photocatalytic activity. Applied Surface Science, 2015, 343, 181-187.	6.1	37
47	Design of flexible resistance sensor based on mesh convex microstructure. Journal Physics D: Applied Physics. 0	2.8	0